Classifying papers according to their light scatter properties

Kathrin HAPPEL, Philipp URBAN, Edgar DÖRSAM and Xaver LUDEWIG
Institute of Printing Science and Technology, Technische Universität Darmstadt

Abstract

Light scatter in paper plays an important role for predicting the color of printed halftones. In this work we measured and evaluated *edge spread functions* for a set of 12 papers. We found, that the light scatter properties of the papers can be classified to only a small number of *light scatter classes*. The light scatter class could be useful information for fitting existing printer models to a printer setup or developing new printer models.

1. Introduction

Light scatter in paper plays an important role for color prediction of printed halftones. Scattered light within the paper bulk causes the so-called *optical dot gain* (ODG) or Yule-Nielsen-effect. It is consensus within the scientific community that modeling ODG is a key element of an accurate printer model and, therefore, a prerequisite for accurate color printing. The detailed knowledge of light scatter within paper can improve the accuracy of printer models and reduce the number of training colors to fit the model to the printer.

In a previous work, we proposed an apparatus and method for measuring local anisotropic light scatter within graphic art papers for predicting ODG, see Happel et al. (2010). The setup is an enhancement of existing approaches which allows for a more robust determination of the light's *point spread function* (PSF).

In this work we investigated *edge spread functions* (ESF) for a set of 12 papers that were detected with a slightly changed measurement setup; PSFs were not calculated. From the results we conclude that a general classification of papers into *light scatter classes* (LSC) is feasible. We believe that this can be useful information for fitting existing printer models to a printer setup or developing new printer models, see Arney et al. (1996).

2. Measurements

The measurement setup consists of a microscope where we placed a razor blade into the light path (see Figure 1a). This allows us to project an edge-shaped illumination onto the sample. A lens system can be utilized for focusing the projection of the razor blade on the sample surface. Furthermore, we enhanced the sample focus by introducing a sample holder, where the sample surface and a reference, in this case a first surface (FS) mirror, are aligned in one plane that is parallel to the microscope stage. This allows us to adjust the focus using the FS mirror and then slide the sample holder to the sample without leaving the focus. A second advantage is that we can use the edge projected onto the reference as the edge that is "best to achieve" considering the optical transfer function of the setup. All measurements are performed relative to this reference edge. The sample holder allows a rotation of the sample to analyze anisotropic scattering.

Images are captured with a camera for each sample and the reference. The edge of the razor blade is aligned to the pixel columns of the camera. This allows us to average over the pixel rows

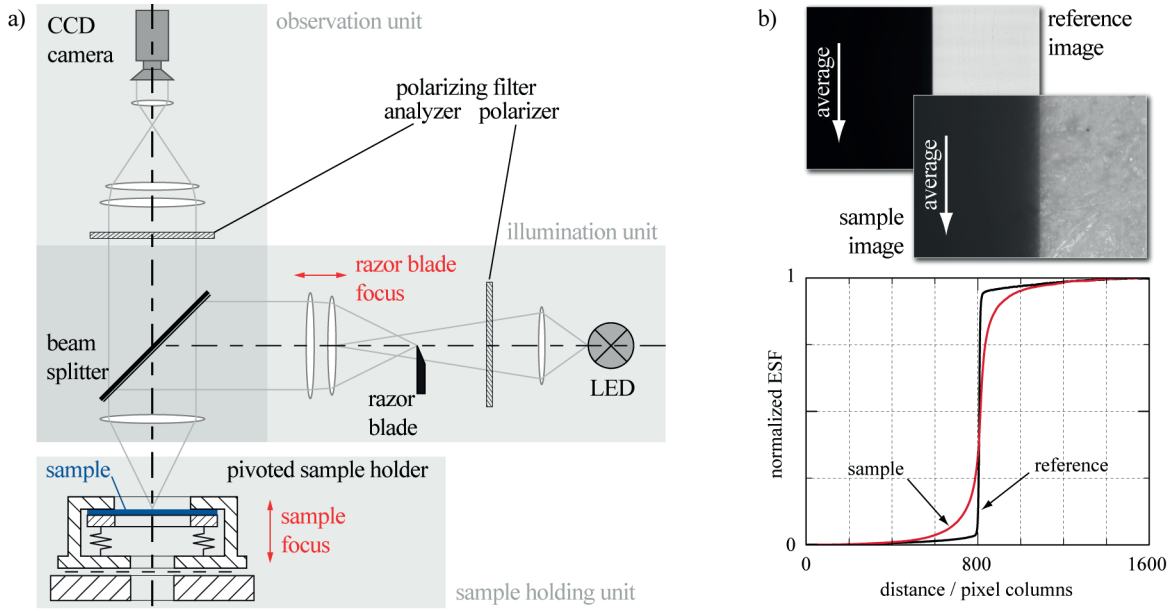

Figure 1. a) Measurement setup; b) Averaging the captured images of reference and sample to ESFs.

to reduce the noise of our measurements, receiving ESFs for all samples and the reference (see Figure 1b).

With a special computation algorithm presented by Happel et al. (2010), we can extract the PSF out of the captured ESFs assuming isotropic light scatter. We found that scatter in paper is almost isotropic. This is also valid for the papers examined here.

In contrast to previous measurements with a halogen lamp, we changed the illumination to a green narrow band LED. This reduces the adverse effect of chromatic aberration on focusing. We chose an LED with a maximum emission at 530 nm. That takes into account that the luminous efficiency function $V(\lambda)$ has its maximum at 555 nm. We changed the previous 8 bit RGB CMOS camera to monochrome CCD with 12 bit depth. In addition, two polarizing filters, located in illumination and observation path respectively, prevent capturing surface reflections. The changes to the previous setting in brief:

1. Green LED - narrow band illumination,
2. Monochrome CCD camera for detection, and
3. Polarizing filters for omitting surface reflections.

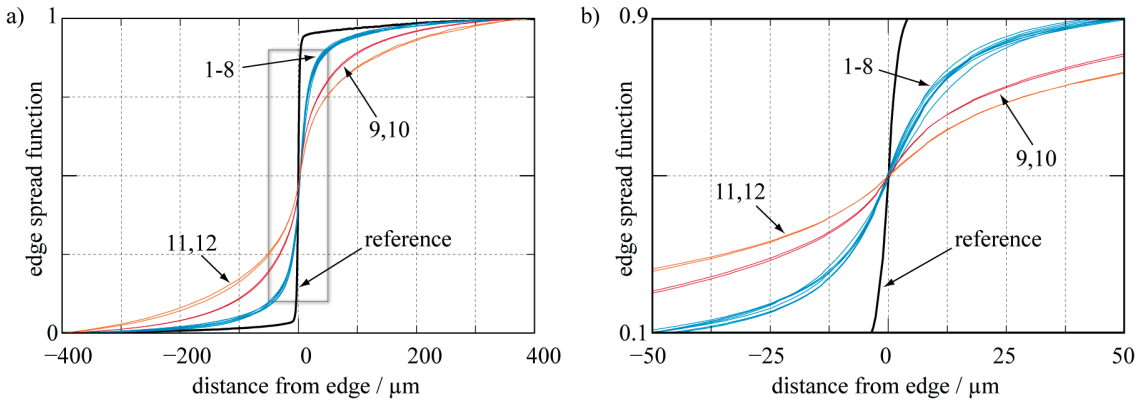

Figure 2. ESFs (a) and their magnification (b) of reference (black) and different samples: inkjet photo papers swellable (red) and microporous (orange), fine art papers (blue); Numbers indicating the paper sample according to Table 1.

For one sample, we capture the edge projection in six angles with 30° distance, covering a total angle of 180°. At each angle, we take five captures. One paper sample is always represented by three specimens. All images are averaged to one single measurement. This reduces disturbing effects of noise caused by illumination changes or thermal effects and of inhomogeneities of the paper, either angular or lateral.

We performed a series of measurements on 12 papers (see Table 1) including four inkjet photo papers (swellable and microporous, matte and glossy coated) and eight fine art papers of two paper series (matte and glossy coated, different paper weights).

3. Results

The different ESFs, obtained by the measurements, can be found in Figure 2a. The ESFs are normalized to an interval of 0-1. Also, for better comparability, the location, where the ESF takes the value 0.5 is set to x=0, indicating the distance from edge.

From the measurement results, we can clearly distinguish three different paper classes. The differently coated fine art papers (blue) are the closest to the reference edge (black). Within this class, there is only little divergence of the ESFs. A noticeably bigger deviation from the reference ESF can be found for the *inkjet papers*. Obviously, the coating of these papers has much larger scatter properties than typical paper ingredients. In addition, the swellable and microporous papers can be distinguished easily. The dependence of the surface gloss on the ESF is negligible.

In Figure 2b, a magnification of the *fine art samples* shows, that the differences in this group are small. There are no significant dependencies between paper weight and scatter properties among the samples of the two fine art paper series. The differences among the measured ESFs might also result from measurement noise or paper inhomogeneities.

Table 1. Papers of the research.

No.	Producer	Series	Coating	Paper weight (g/m²)	LSC
1	Scheufelen	Consort Royal	glossy	115	1
2	Scheufelen	Consort Royal	glossy	250	1
3	Scheufelen	Consort Royal	matte	115	1
4	Scheufelen	Consort Royal	matte	250	1
5	Scheufelen	BVS	glossy	100	1
6	Scheufelen	BVS	glossy	250	1
7	Scheufelen	BVS	matte	100	1
8	Scheufelen	BVS	matte	250	1
9	Felix Schöller	PE-Photopaper (swellable)	glossy	230	2
10	Felix Schöller	PE-Photopaper (swellable)	matte	230	2
11	Felix Schöller	PE-Photopaper (microporous)	glossy	240	3
12	Felix Schöller	PE-Photopaper (microporous)	matte	240	3

3.1 Light Scatter Classes

The papers investigated can be categorized into three *light scatter classes* (LSC): 1. Little Scatter (fine art papers), 2. Medium Scatter (inkjet swellable), and 3. Large Scatter (inkjet microporous). It seems to be reasonable that a general classification of papers due to their scatter properties is possible. Such an LSC could be included into the papers' data sheets. The ODG property of a paper could directly be deduced from its LSC. This could simplify modeling printing systems or

fitting printer models to a given printer setup. LSCs can be incorporated especially into first principle models as presented in Wyble and Berns (2000).

For instance, Arney et al. (1996) proposed to replace the Yule-Nielsen n-factor by two variables, one of them (w) is referring to light scatter in paper. He found an analytical representation of this variable w:

$$w = 1 - \exp\left(-A\, k_p f\right)$$

where A characterizes the halftone geometry, f is the halftone dot frequency, and k_p is a constant that is proportional to the mean distance of light scatter. This parameter k_p could directly be deduced from the LSC.

4. Outlook

In future research, additional papers will be measured, including other inkjet and fine art papers, but also uncoated papers and special papers. A database of papers and their scatter properties shall be created. With these results the definition of scatter classes could be enhanced. Additionally, we study how to enhance existing printer models with the results from our measurements, e.g. how to relate the Yule-Nielsen n-factor to the light scatter properties or the LCS of the paper.

Acknowledgments

The authors thank Manfred Jakobi and Karsten Rettig for their electrical and mechanical constructions on the measurement setup.

References

Happel, K., M. Walter, P. Urban, and E. Dörsam. 2010. Measuring Anisotropic Light Scatter within Graphic Art Papers For Modeling Optical Dot Gain. In *IS&T/SID Color and Imaging Conference*, *Proceedings.* San Antonio, 347-352.

Wyble, D.R., and R.S. Berns. 2000. A critical review of spectral models applied to binary color printing. *Color Research and Application* 25 (4): 4-19.

Arney, J., C. Arney, and P. Engeldrum. 1996. Modeling the Yule Nielsen Halftone Effect. *Journal of Imaging Science and Technology* 40 (3): 233-238.

Address: Kathrin Happel, Institute of Printing Science and Technology, Technische Universität Darmstadt, Magdalenenstr. 2, 64289 Darmstadt, Germany
E-mails: happel@idd.tu-darmstadt.de, urban@idd.tu-darmstadt.de, doersam@idd.tu-darmstadt.de, ludewig@idd.tu-darmstadt.de